

# Dynamics and Control of Lattice Beams Using Simplified Finite Element Models

D.T. Berry,\* T.Y. Yang,† and R.E. Skelton‡  
*Purdue University, West Lafayette, Indiana*

Simple beam finite element analysis models for a flexible lattice beam with repetitive geometry are developed using the strain and kinetic energies formed by replacing the lattice with an equivalent continuum. This beam element has six degrees of freedom at each of its two nodes. The performance of the simple finite element formulation in free vibration analysis is evaluated by comparison with free vibration results of a full or complex finite element model of the lattice formed by using truss bar elements. Modal Cost Analysis is performed on the modes obtained using both the simple analysis and complex models and the results are compared. Based on this information, model reduction decisions are influenced by the control objectives. A set of reduced order controllers are designed based upon the resulting reduced order models. These controllers are used to control an evaluation model based on the full complex model. For low control energies, these controllers perform well when compared with the optimal controller based on the evaluation model itself. The example analysis shows that the simple finite element analysis models can be used with accuracy in the control law design process for lattice beams with low bandwidth controllers.

## Introduction

THE dynamics and control of lattice structures has attracted increasing attention recently due to their possible use in space applications. Structural and control design analyses of these lattices must be highly reliable since they cannot be tested full scale in their operational environment prior to flight. Furthermore, simplified structural modeling techniques will be needed due to the size of these structures. For example, a full finite element analysis using truss bars of a structure containing large numbers of elements and nodes may be uneconomical, especially during the initial design phases when the structure and its associated systems are subject to change. At the same time, the structure's high flexibility requires a relatively large number of vehicle elastic modes to be accurately predicted. The controls analyst may also require accuracy in the structure's high-frequency modes rather than just those of low frequency.

This paper describes techniques that result in simple structural analysis models containing the dynamic information of the full complex model without the need for direct analysis on the complex model itself. Specifically, "simple finite element analysis" models based upon an equivalent continuum of a given lattice beam are developed. To evaluate the accuracy of these finite element analysis models, natural frequencies and mode shapes are compared to those of a complete truss bar element model of the structure (the "complex model"). The accuracy of the simple analysis models is good especially when the half-wavelength of a mode spans many repeating cells. These simple analysis models will also be used as a basis for control law design after modal truncation using modal cost analysis is performed. The resulting reduced order models will be called the "control design models." It will be shown that even the design model containing only one mode may yield a

satisfactory control law design, depending on the control accuracy requirements.

A graphic outline of the paper is shown in Fig. 1. A typical beam-like lattice structure is idealized as an equivalent continuum Timoshenko beam. The strain and kinetic energies of this continuum are used to formulate a 12 degree-of-freedom (dof) beam finite element. This element is used to produce a set of "simple finite element analysis models" of the lattice containing 1-10 equal length elements. Free vibration analysis is performed on these simple analysis models and the results are compared with a full truss bar element model of the complete lattice grid. This full model will be referred to as the "complex model." The simple analysis models and the complex model are analyzed using Modal Cost Analysis (MCA) in order to judge the importance of the various modes in a given control problem. Modal truncation decisions are made at this point by retaining those modes having the largest modal cost. The resulting models are called the reduced-order "control design models." Control laws are designed based on these control design models using Linear Quadratic Gaussian (LQG) control theory. These control laws are used to control an evaluation model constructed from the complex model. The evaluation of these control laws proceeds as shown in Fig. 2. The result of this analysis is the performance plot also outlined in Fig. 2. It is essentially a plot of the magnitude of the output variable  $y$  vs the magnitude of the input control variable  $u$ . Using the performance plot, the usefulness and accuracy of the simple analysis models based on the equivalent continuum and used in control law design are evaluated.

## Structural Modeling

The lattice beam model chosen for analysis is a 10 bay, simply supported beam with a repeating cell of the "single-bay, double-lace" type. The geometry of the cell is shown in Fig. 3. Three different types of bars are used in the lattice: longitudinal, diagonal, and batten bars. The geometry and material characteristics of these bars are listed in Fig. 3. Overall length of the lattice beam is 75 m. The lattice beam has 33 nodes and 123 bars. Although a lattice beam with more repeating cells could easily be modeled, it is shown later that the ten cell lattice has enough beam-like and nonbeam-like behavior to illustrate the proposed method.

Presented as Paper 84-1043 at the AIAA Dynamics Specialist Conference, Palm Springs, Calif., May 17-18, 1984; submitted July 23, 1984; revision received Dec. 7, 1984. Copyright © American Institute of Aeronautics and Astronautics, Inc., 1984. All rights reserved.

\*Graduate Research Assistant, School of Aeronautics and Astronautics. Student Member AIAA.

†Professor and Dean, Schools of Engineering. Associate Fellow AIAA.

‡Professor, School of Aeronautics & Astronautics. Member AIAA.

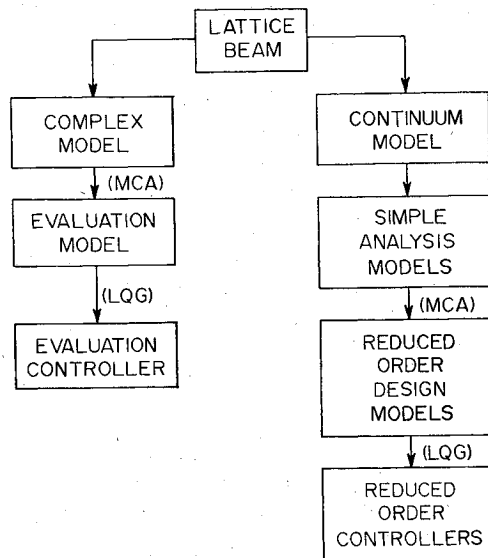


Fig. 1 Block diagram of the modeling process.

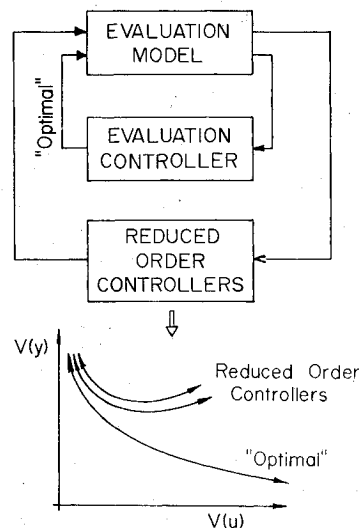
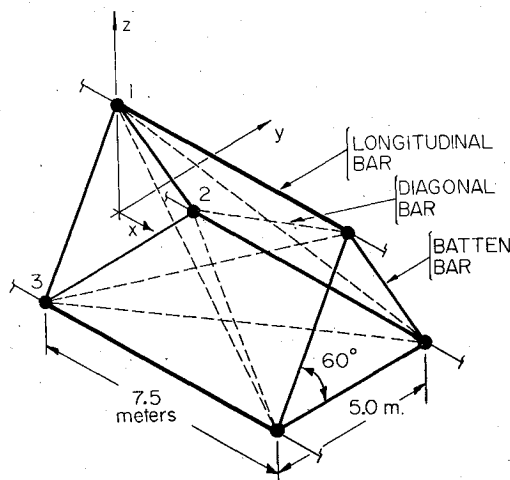


Fig. 2 Block diagram of the evaluation process.



BARS	$E (\frac{N}{m^2})$	$A (m^2)$	$\rho (\frac{kg}{m^3})$
LONGITUDINAL	$71.7 \times 10^9$	$80. \times 10^{-6}$	2768.
DIAGONAL	$71.7 \times 10^9$	$40. \times 10^{-6}$	2768.
BATTEN	$71.7 \times 10^9$	$60. \times 10^{-6}$	2768.

Fig. 3 Repeating cell geometry: single bay, double-lace lattice beam.

The complex model is produced by using axial truss bar elements of the type shown in Fig. 4. The equations for a representative bar are

$$\frac{\rho AL}{6} \begin{bmatrix} 2 & & & & & \\ & 0 & 2 & & & \\ & 0 & 0 & 2 & & \\ & 1 & 0 & 0 & 2 & \\ & 0 & 1 & 0 & 0 & 2 \\ & 0 & 0 & 1 & 0 & 0 & 2 \end{bmatrix} \begin{Bmatrix} \ddot{u}_1 \\ \ddot{v}_1 \\ \ddot{w}_1 \\ \ddot{u}_2 \\ \ddot{v}_2 \\ \ddot{w}_2 \end{Bmatrix} + \frac{EA}{L} \begin{bmatrix} S & -S \\ -S & S \end{bmatrix} \begin{Bmatrix} u_1 \\ v_1 \\ w_1 \\ u_2 \\ v_2 \\ w_2 \end{Bmatrix} = \begin{Bmatrix} F_{x1} \\ F_{y1} \\ F_{z1} \\ F_{x2} \\ F_{y2} \\ F_{z2} \end{Bmatrix} \quad (1)$$

where

$$S = \begin{bmatrix} c_\beta^2 c_\alpha^2 & & \text{sym} \\ c_\beta^2 c_\alpha s_\alpha & c_\beta^2 s_\alpha^2 & \\ c_\beta s_\beta c_\alpha & c_\beta s_\beta s_\alpha & s_\beta^2 \end{bmatrix} \quad (1a)$$

$c_\alpha = \cos \alpha$ ,  $c_\beta = \cos \beta$ ,  $s_\alpha = \sin \alpha$ ,  $s_\beta = \sin \beta$ , and  $L$  is the length of the truss bar element. A consistent mass formulation has been used. Each bar in the lattice is modeled using one such element. The complex model has a total of 99 dof. The equations of motion for the assembled structure are of the following symbolic form

$$[M] \{\ddot{q}\} + [K] \{q\} = \{F\} \quad (2)$$

The simple finite element models are produced using the strain and kinetic energies of a Timoshenko beam continuum which is "equivalent" to the full lattice. Here, "equivalence" means that the lattice and the continuum contain equal kinetic and strain energies when both are subjected to the same displacement and velocity fields. The method used to produce the continuum model is presented in Ref. 1. Briefly, the technique involves developing expressions for the strain and kinetic energies of a repeating lattice cell as functions of displacement and strain components along the centerline. These strain components are then expanded in a Taylor's series about a suitably chosen origin. In general, terms up to the second order in the Taylor's series expansion must be kept to allow internal deformations within a repeating cell to be accounted for correctly. As pointed out in Ref. 1, however, the single-bay, double-laced lattice cell needs only the terms in the zeroth order of the Taylor's series strain expansion. This is, in effect, an assumption of a uniform state of strain across each repeating cell. This means that the half-wavelength of a structural mode must contain a reasonable number of repeating cells for that mode to be predicted accurately. Following the Taylor's series expansion, arguments are given that reduce the number of independent displacement and strain components. The numerical coefficients on the remaining components become the stiffness and mass coefficients of the equivalent continuum. They are calculated explicitly in Ref. 1 for several lattice beam geometries, including the one used here. The strain energy has the form

$$u = \frac{1}{2} \bar{L} \{\epsilon\}^T [C] \{\epsilon\} \quad (3)$$

Table 1 Natural frequencies<sup>a</sup> of the simply supported lattice beam models

Mode No.	Mode	Number of simple finite flements					Analytic solution <sup>b</sup>	Complex Model
		1	2	3	5	10		
1,2	1st bending	12.98	11.45	11.38	11.35	11.34	11.34	11.44
4,5	2nd bending		51.52	43.35	42.17	41.72	41.56	42.90
8,9	3rd bending			114.5	87.81	84.42	83.24	88.40
11,12	4th bending				146.2	134.8	130.5	142.4
15,16	5th bending				306.4	191.2	180.0	201.1
21,22	6th bending					252.9	230.2	261.2
24,25	7th bending					319.5	280.4	318.6
26,27	8th bending					387.1	330.3	367.8
29,30	9th bending					444.4	379.9	401.6
3	1st torsion		43.71	41.47	40.30	39.81	39.64	39.55
7	2nd torsion			92.73	84.55	80.60	79.29	78.05
10	3rd torsion				136.0	123.6	118.9	116.3
13	4th torsion				190.5	169.1	158.6	152.2
14	5th torsion					218.6	198.2	185.2
17	6th torsion					272.0	237.9	214.5
19	7th torsion					327.8	277.5	238.9
20	8th torsion					381.0	317.2	257.3
23	9th torsion					421.6	356.8	268.8
6	1st axial	86.67	80.63	79.50	78.98	78.68	78.60	78.05
18	2nd axial		281.7	260.0	244.6	238.0	235.6	235.2
28	3rd axial			471.7	433.3	403.2	393.0	395.3

<sup>a</sup>Units are radians per second. <sup>b</sup>Analytic solution is of an equivalent homogeneous Timoshenko beam.<sup>5</sup>

where  $\{\epsilon\}$  are the beam-like strain components ( $6 \times 1$ ),  $\bar{L}$  is the length of a repeating cell, and  $[C]$  are the stiffness coefficients of the equivalent continuum ( $6 \times 6$ ). The kinetic energy is similarly represented as shown

$$T = \frac{1}{2} \bar{L} \{\dot{u}\}^T [M] \{\dot{u}\} \quad (4)$$

where  $\{u\}$  are the beam-like displacement components ( $6 \times 1$ ), and  $[M]$  are the inertia coefficients of the equivalent continuum ( $6 \times 6$ ). For the lattice beam shown in Figs. 3, the equivalent continuum is homogeneous and isotropic so that matrices  $[C]$  and  $[M]$  are diagonal and the stiffness properties in the  $xy$  and  $xz$  planes are equal. The stiffness and mass properties of the equivalent continuum are as follows:

Bending rigidity	$EI = 8.011 \times 10^7 \text{ N} \cdot \text{m}^2$	
Axial rigidity	$EA = 2.528 \times 10^7 \text{ N}$	
Shear rigidity <sup>§</sup>	$GA = 2.203 \times 10^6 \text{ N}$	
Torsional rigidity	$GJ = 9.178 \times 10^6 \text{ N} \cdot \text{m}^2$	
Mass per unit length	$\rho A = 1.795 \text{ kg/m}$	
Rotatory inertia coefficient	$\rho I = 5.123 \text{ kg} \cdot \text{m}$	
Torsional inertia coefficient	$\rho J = 10.246 \text{ kg} \cdot \text{m}$	(5)

Once the strain and kinetic energies of the continuum are known as functions of the constants listed in Eq. (5), finite element models are generated using a set of suitable displacement functions and Castigliano's theorem. As shown in Fig. 5, the simple finite element formulated is a 12 dof prismatic bar element with shear and rotatory inertia effects included. The shear and rotatory inertia are included in the same fashion as that by Archer.<sup>3</sup> The matrix equations of motion for the beam

<sup>§</sup>In Ref. 2, an incorrect value of  $GA = 2.203 \times 10^7 \text{ N}$  was used. The value of shear rigidity has an effect on the data in Table 1 and Figs. 9, 10, and 11 of that paper. The corrected data are given in the present paper.

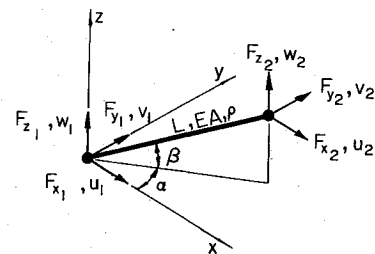


Fig. 4 Axial force bar element used in complex model.

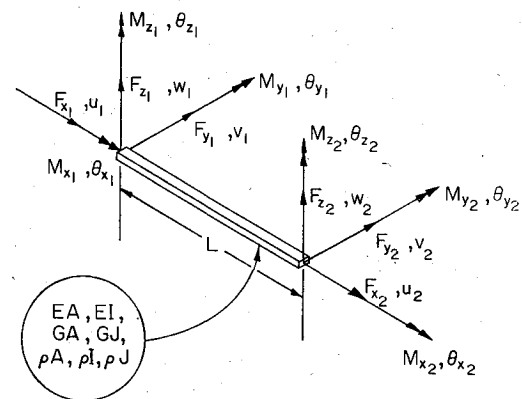


Fig. 5 Prismatic bar finite element used in simple analysis models.

finite element can be obtained by using Lagrange's equations

$$\frac{d}{dt} \left( \frac{\partial T}{\partial \dot{q}_i} \right) + \frac{\partial U}{\partial q_i} = F_i \quad (6)$$

where  $T$  and  $U$  are the strain and kinetic energies of the continuum in terms of the beam element dof. These are obtained by using Eqs. (3) and (4) and the displacement functions for a Timoshenko beam.<sup>3</sup> The resulting equations take the form

$$[M] \{\ddot{q}\} + [K] \{q\} = \{F\} \quad (7)$$

**Table 2 Reduced-order design models**

Reduced-order model no.	Reduced from which model	Mode no. retained	Cost perturbation index
Evaluation	Complex	1,8,15,24,29	0.9997
1	1 element analysis	1	0.9940
2	5 element analysis	1,8	0.9996
3	10 element analysis	1,8,15,24	0.9999

These are identical in form to the equations listed in Ref. 4 for a 12 dof homogeneous, isotropic Timoshenko beam.

Ten models with 1-10 equal length beam elements are constructed. The number of dof in each model varies from 12 in a one-element model to 66 in a 10-element model. If it is known beforehand that only, say, bending motions are observable in the output vector of interest, axial and torsional dof may be discarded leading to much smaller models. Modal Cost Analysis, the model reduction technique used in this paper, will do this automatically, however. The homogeneous, undamped equations of motion for the various models are of the form

$$[M]\{\ddot{q}\} + [K]\{q\} = \{0\} \quad (8)$$

### Free Vibration Analysis

To evaluate the performance of the present formulation, free vibration analysis is performed on the simple analysis and complex models. Since the complex model does not have a node at its centerline, a multipoint constraint procedure is used. For example, if the average  $v$  displacement in the  $y$  direction of the end cross section (which contains nodes 1-3 as shown in Fig. 3) is to be constrained, an equation of the form

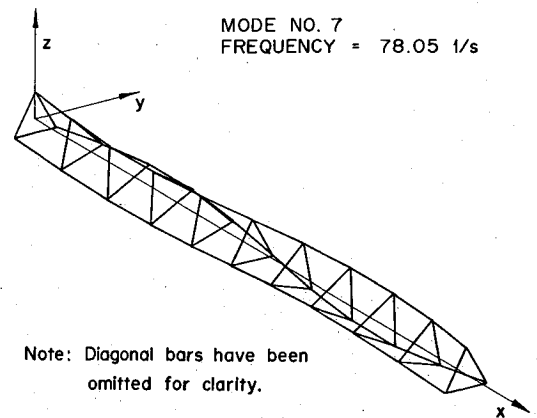
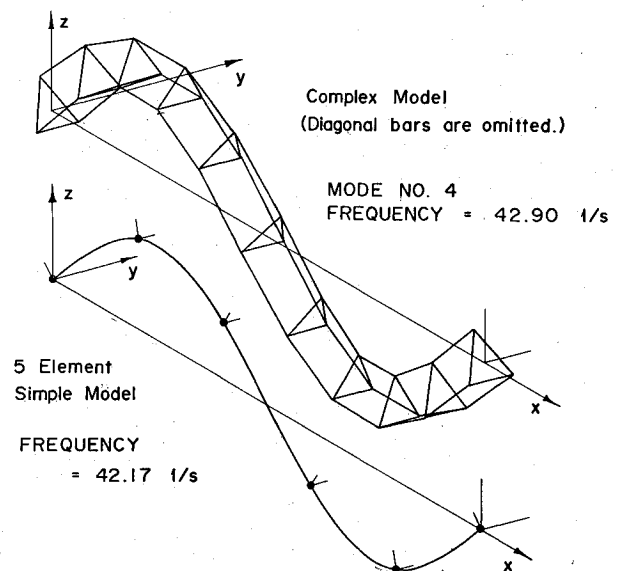
$$v_1 + v_2 + v_3 = 0 \quad (9)$$

is written. This equation is used to express one of the displacements in terms of the others. The equations are substituted into the equations of motion for the lattice and the dependent dof is eliminated. Nine constraint equations of the form of Eq. (9) are needed to enforce the nine simply supported boundary conditions. The constrained complex model has 90 dof. The equations of motion for all of the models in free vibration are of the form

$$[-\omega^2 [M] + [K]]\{\phi\} = \{0\} \quad (10)$$

Natural frequency results for the lattice beam example are shown in Table 1. Seven different models are used: 1) complex truss bar model, 2) five simple finite element analysis models with 1, 2, 3, 5, and 10 elements per model, and 3) an analytical solution of an equivalent homogeneous Timoshenko beam.<sup>5</sup> These data show that frequencies of the simple models converge to the equivalent Timoshenko beam frequencies of the continuum as the number of simple finite elements increases.

The rest of the data shows the comparison between the simple analysis models and the complex model of the lattice. It is noted that the complex model has approximately 30 beam-like modes. The term "beam-like" is used here to refer to bending, axial, and torsional behavior of the complex model. The second torsional and second bending modes are plotted in Figs. 6 and 7. The 30 beam-like modes are those with the lowest frequencies. The highest 60 modes are, for the most part, nonbeam-like modes that cannot be predicted by the simple models. Furthermore, the size of the complex model (90 dof) indicates that these upper 60 modes cannot be very accurate. They all have a frequency above 89 Hz while the beam-like modes all have frequencies below 64 Hz. Modes were iden-

**Fig. 6 Sample complex model torsional mode.****Fig. 7 Sample complex and simple model bending mode.**

tified strictly based upon their plotted shapes. While it is true that even the mode labeled as the first bending mode contains local nonbeam-like effects (for example, distortion of the cross section in its own plane), these modes are characterized as "beam-like" and are compared to the modes of the simple analysis models. Figure 7 shows the second bending mode for the complex model and the second bending mode for the simple analysis model containing five elements. Both modes have been normalized by their respective mass matrices. No unequal scaling was done for one mode relative to the other. The displacement functions used to generate the simple finite elements were used to interpolate values for the displacement between nodes. The rest of the beam-like modes have been plotted and match those of an equivalent simple analysis model. The 30 pairs of beam-like modes are given in Ref. 6.

Several comments can be made at this point about the comparison between the frequencies generated by the two models. First, the continuum model overestimates the stiffness in bending and underestimates the stiffness in torsion. This is due to additional nonbeam-like lattice effects that are not represented in the continuum model. Furthermore, although low-order bending, axial, and torsional frequencies are predicted quite accurately, the accuracy of the bending and torsional frequencies decreases for the higher modes. This occurs because the half-wavelength of the higher modes span fewer repeating cells, so the assumptions made in the development of the continuum are violated. For example, the half-

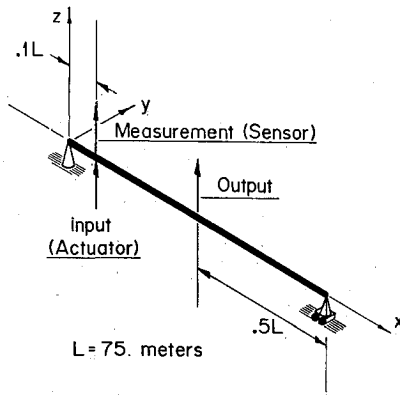


Fig. 8 Schematic of example control problem.

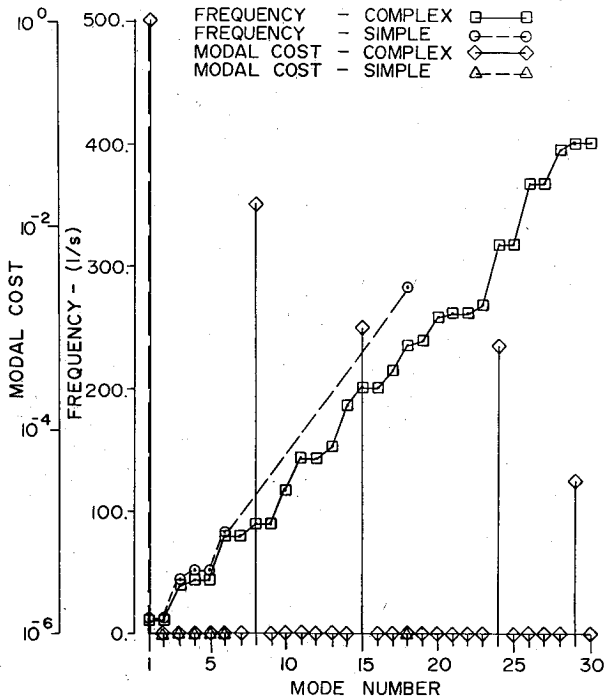


Fig. 9 Modal cost and frequency data for complex model and two-element analysis model.

wavelength of the  $n$ th mode spans  $10/n$  repeating cells. As the number of cells per half-wavelength decreases, the strain gradients increase so the Taylor's series expansion becomes less accurate. Physically, the nonbeam-like behavior of the lattice becomes important in the higher modes. This behavior cannot be predicted with a Timoshenko-type beam model. The negative of the statement above is also true; as the number of cells per half-wavelength increases, the strain gradients decrease, so the Taylor's series expansion becomes more accurate. The method is developed for handling lattice beams with considerably more cells than the example presented here. In fact, the simple models are developed specifically for use in the simultaneous structural and control optimization of structures with relatively large numbers of dof.

### Modal Cost Analysis

The aim of this study is to develop reduced-order controllers based on the simple finite element analysis models and to use these controllers to control an evaluation model based on the full complex model. Model reduction of the complex model to an evaluation model is needed due to the large size of the complex model. The issue of model reduction is, therefore, con-

sidered. Modal Cost Analysis is used to evaluate the importance and contribution of each mode in a given control problem.

Modal Cost Analysis is presented in detail in Refs. 7 and 8. It is a method that determines the importance of a particular mode to a given control problem. While the details are available in the above mentioned references, a brief description is given here. The total cost function

$$V(y) = \lim_{t \rightarrow \infty} \frac{1}{t} E \left\{ \int_0^t \|y(\tau)\|_Q^2 d\tau \right\} = \sum_{i=1}^n V_i \quad (11)$$

where  $E$  is the expected value operator and  $V_i$  the cost associated with the  $i$ th mode.  $V_i$  is defined by

$$V_i = \text{tr} \lim_{t \rightarrow \infty} \frac{1}{t} E \left\{ \int_0^t \frac{\partial}{\partial x_j} \|y(\tau)\|_Q^2 x_i d\tau \right\}, x_i = \begin{Bmatrix} \eta_i \\ \dot{\eta}_i \end{Bmatrix} \quad (12)$$

where  $\eta_i$  is the  $i$ th modal coordinate,  $V_i$  are the modal costs, and  $\text{tr}$  is the matrix trace operator.

$V_i$  can be written in terms of modal data. Let the system be represented by the following matrix second-order equations:

$$[M] \{\ddot{q}\} + [D] \{\dot{q}\} + [K] \{q\} = [B] \{u + w\}$$

$$\{y\} = [C] \{q\} + [C'] \{\dot{q}\}$$

$$\{z\} = [Z] \{q\} + [Z'] \{\dot{q}\} + \{v\} \quad (13)$$

The forcing term is a control input from noisy actuators. The measurement also includes noise. The transformation to modal coordinates is made by using the modal matrix associated with the undamped, homogeneous system equations

$$\{q\} = [\Phi] \{\eta\} \quad (14)$$

The modal matrix  $[\Phi]$  is normalized with respect to the system mass matrix. After premultiplying by  $[\Phi]^T$ , the resulting equations are

$$\{\ddot{\eta}\} + [\Phi]^T [D] [\Phi] \{\dot{\eta}\} + [\omega_i^2] \{\eta\}$$

$$= [\Phi]^T [B] \{u + w\}$$

$$\{y\} = [C] [\Phi] \{\eta\} + [C'] [\Phi] \{\dot{\eta}\}$$

$$\{z\} = [Z] [\Phi] \{\eta\} + [Z'] [\Phi] \{\dot{\eta}\} + \{v\} \quad (15)$$

where  $\{\eta\}$  is an  $n \times 1$  vector ( $n$  is the number of modes in the model). Although damping must be included in the system equations, it is a highly uncertain parameter. It is assumed small for the present structure and has the form

$$[\Phi]^T [D] [\Phi] = [2\zeta_i \omega_i] \quad (16)$$

The modal damping ratio  $\zeta_i = 0.005$  for all modes. Defining

$$[b_i^T] = \text{ith row of } [\Phi]^T [B]$$

$$\{c_i\} = \text{ith column of } [C] [\Phi]$$

$$\{c_i'\} = \text{ith column of } [C'] [\Phi] \quad (17)$$

it can be shown<sup>7</sup> that for a system in the above form, the modal cost  $V_i$  associated with the mode  $x_i$  is given by

$$V_i = \frac{1}{4\zeta_i \omega_i^3} [\|c_i\|_Q^2 + \omega_i^2 \|c_i'\|_Q^2] \|b_i\|_W^2 \quad (18)$$

where the notation  $\|c_i\|_Q^2 = \{c_i\}^T [Q] \{c_i\}$  is used.  $[Q]$  is a weighting matrix on the outputs and  $[W]$  the intensity of the actuator noise. Note that the  $V_i$  are defined strictly in terms of modal data. That is,  $\{c_i\}$ ,  $\{c'_i\}$ , and  $\{b_i\}$  are composed of the values of the  $i$ th mode shape at the input and output locations, respectively.

MCA is used to reduce the size of the simple analysis models. The resulting models are called control design models. A set of reduced-order controllers is then designed from these control design models. MCA will also be used to reduce the total set of complex model modes to an evaluation model that will be used to assess the performance of the reduced-order controllers.

### Results of Modal Cost Analysis

The results of the Modal Cost Analysis are now used to evaluate the importance of the modes of the complex model and of the simple analysis models in a particular control problem. The control problem analyzed is illustrated graphically in Fig. 8. A single force actuator is located at a distance of 7.5 m from one end of the simply supported lattice beam. It is located at the top vertex of that particular triangular cross section and drives the  $z$  direction. The noise in the actuator is assumed to be uncorrelated Gaussian white noise with intensity  $[W] = 1.0 \times 10^{-4} \text{ N}^2$ . The sensor is located at the same point and measures the displacement in the  $z$  direction. Noise in the sensor is assumed to be uncorrelated Gaussian white noise with intensity  $[V] = 1.0 \times 10^{-10} \text{ m}^2$ . The controlled output variable  $y$  is the displacement in the  $z$  direction at the top vertex of the midspan cross section. The sensor, actuator, and output for the simple analysis models are located at equivalent axial stations and measure the same displacements in the same directions. For this example,  $[Q] = 1.0$ . These examples have been constructed so that only the lateral  $z$  direction bending modes will have significant modal costs.

Modal costs of the complex model modes and the simple analysis model modes generated with 2, 5, and 10 elements per model are shown in Figs. 9-11, respectively. The modal cost data have been normalized so that the maximum modal cost has a value of 1.0. Costs below  $1.0 \times 10^{-6}$  are set to this value. Several comments are in order about these Figures. First, not every analysis model predicts every complex mode. As the number of elements in the analysis models increases, the number of modes predicted also increases. Second, the analysis model frequencies do not monotonically increase with mode number. They have been reordered to show the equivalence with the complex model modes. Third, only the odd bending modes have significant modal costs because the output location is at a node of the even-numbered modes. These modes are unobservable for this particular output location. That is, their modal costs are zero. Thus, these modes have no contribution to the cost function and can be dropped from any control design model. If a two-mode model were needed, traditional modal truncation based on frequency would keep bending modes 1 and 2, which is no better than a one-mode model of mode 1 since mode 2 has no effect on the output. Therefore, model reduction decisions cannot be divorced from the control objectives.

Figures 9-11 show that, when compared with the complex model, the analysis models accurately predict the modal costs of the complex model for the lowest modes. Equation (18) shows that modal costs are inversely proportional to the cube of the natural frequency, so the simple models predict slightly higher modal costs due to their slightly lower frequencies. These higher modal costs would indicate that, for example, the third bending mode is more important to the minimization of the cost function than it actually is. It is noted, however, that the trends of the modal cost data are accurately predicted by the analysis models. That is, modal truncation decisions based upon Modal Cost Analysis of an analysis model will at least preserve the relative importance of the modes of this

analysis model to the overall control objective. It is also noted that as the number of elements in the analysis models increases, the accuracy of the modal costs converges, but that the error does not go to zero. This is to be expected since, although the frequencies of the analysis models converge, they converge to the frequencies of the equivalent Timoshenko beam continuum and not to the frequencies of the complex model (see Table 1).

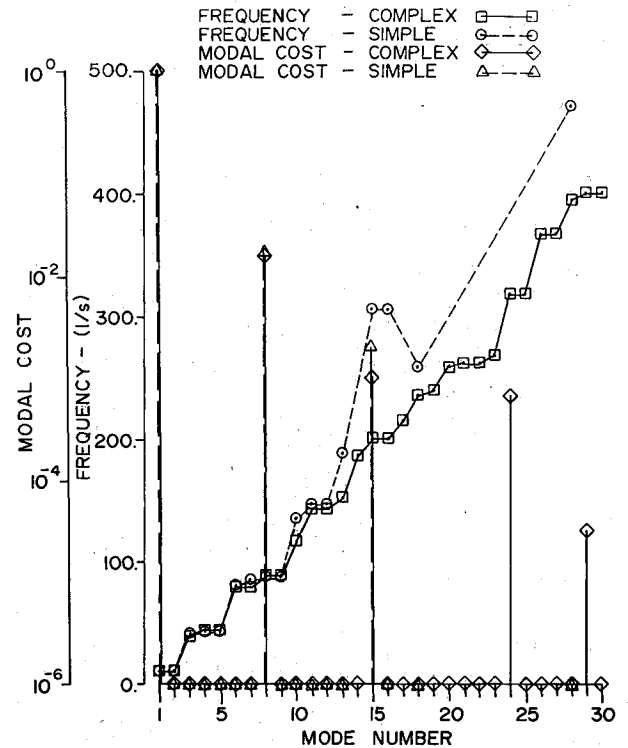


Fig. 10 Modal cost and frequency data for complex model and five-element analysis model.

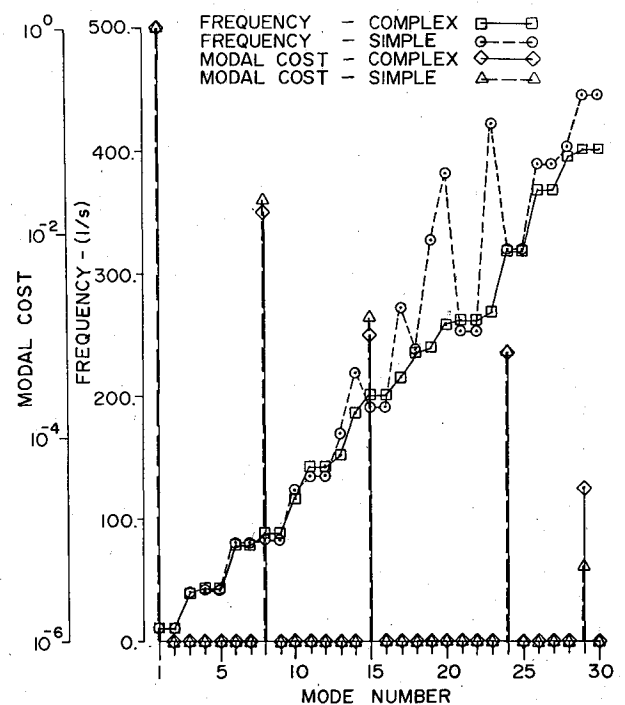


Fig. 11 Modal cost and frequency data for complex model and 10-element analysis model.

### Model Reduction

Model reduction using Modal Cost Analysis is straightforward.<sup>8</sup> For an  $n$  mode, reduced-order design model, the  $n$  modes with the highest modal cost are selected. Based on the information in Figs. 9-11, three reduced-order design models are formed: 1) a one-mode model containing the first bending mode of the two-element analysis model, 2) a two-mode model containing the first and third bending modes of the seven-element analysis model, 3) a four-mode model containing the first, third, fifth, and seventh bending modes of the ten-element analysis model. Modal Cost Analysis is also used in the formation of an evaluation model. This reduced model is needed since the full complex model has too many modes to use as a basis for controller design and evaluation. The evaluation model is constructed from the first, third, fifth, seventh, and ninth bending modes of the complex model.

A measure of how completely a reduced-order model matches the total cost information of its parent model is given by the cost perturbation index (CPI). The CPI is defined as

$$\text{CPI} = \frac{\sum_{i=1}^{\hat{n}} V_i}{V(y)} \quad (19)$$

where  $V(y)$  is the total modal cost and  $\hat{n}$  the number of modes in the reduced-order model. For a reduced model containing all of the cost information of its parent, CPI = 1.0. It is clear that those modes with the smallest  $V_i$  should be deleted. The reduced-order design models and their associated cost perturbation indices are listed in Table 2.

### Reduced-Order Controller Design

All of the reduced-order design models are fully observable and controllable. A controller for each model is designed using Linear Quadratic Gaussian techniques.<sup>9</sup> The equations of motion in state space form are

$$\begin{aligned} \dot{x}_R &= [A_R] \{x_R\} + [B_R] [\{u\} + \{w\}] \\ y &= [C_R] \{x_R\} \\ z &= [Z_R] \{x_R\} + \{v\} \end{aligned}$$

and

$$\begin{aligned} E[w(t)] &= 0 & E[w(t)x_R^T(0)] &= 0 \\ E[v(t)] &= 0 & E[v(t)x_R^T(0)] &= 0 \\ E[w(\tau)w^T(t)] &= [W]\delta(t-\tau) & E[v(t)w^T(\tau)] &= 0 \\ E[v(\tau)v^T(t)] &= [V]\delta(t-\tau) \end{aligned} \quad (20)$$

The cost function to be minimized is

$$V = \lim_{t \rightarrow \infty} \frac{1}{t} E \left\{ \int_0^t (\|y(\tau)\|_Q^2 + \sigma \|u(\tau)\|_R^2) d\tau \right\} \quad (21)$$

The resulting controller is

$$\begin{aligned} \dot{x}_C &= [A_C] \{x_C\} + [F] \{z\} \\ u &= [G] \{x_C\} \\ [G] &= \frac{1}{\sigma} [R]^{-1} [B]^T [K] \\ [F] &= [P] [Z_R]^T [V]^{-1} \\ [A_C] &= [A_R] + [B_R] [G] - [F] [Z_R] \end{aligned} \quad (22)$$

where  $[P]$  and  $[K]$  satisfy the Riccati equations

$$\begin{aligned} [K] [A_R] + [A_R]^T [K] - \frac{1}{\sigma} [K] [B_R] [R]^{-1} [B_R]^T [K] \\ + [C_R]^T [Q] [C_R] &= [0] \\ [P] [A_R]^T + [A_R] [P] - [P] [Z_R]^T [V]^{-1} [Z_R] [P] \\ + [D_R] [W] [D_R]^T &= [0] \end{aligned} \quad (23)$$

This controller is optimal for the reduced-order design model itself, but will not perform optimally when used to drive the evaluation model. The evaluation model can be written

$$\begin{aligned} \dot{x}_E &= [A_E] \{x_E\} + [B_E] [\{u\} + \{w\}] \\ y &= [C_E] \{x_E\} \\ z &= [Z_E] \{x_E\} + \{v\} \end{aligned} \quad (24)$$

The entire closed-loop system has the form

$$\begin{aligned} \dot{x}_a &= [A_a] \{x_a\} + [B_a] \{w_a\} \\ y_a &= [C_a] \{x_a\} \end{aligned} \quad (25a)$$

where

$$\begin{aligned} \{x_a\} &= \begin{Bmatrix} x_E \\ x_C \end{Bmatrix} \\ [A_a] &= \begin{bmatrix} A_E & B_E G \\ F Z_E & A_C \end{bmatrix}, \quad \{y_a\} = \begin{Bmatrix} y \\ u \end{Bmatrix} \\ [C_a] &= \begin{bmatrix} C_E & 0 \\ 0 & G \end{bmatrix} \\ [D_a] &= \begin{bmatrix} B_E & 0 \\ 0 & F \end{bmatrix}, \quad \{w_a\} = \begin{Bmatrix} w \\ v \end{Bmatrix} \end{aligned} \quad (25b)$$

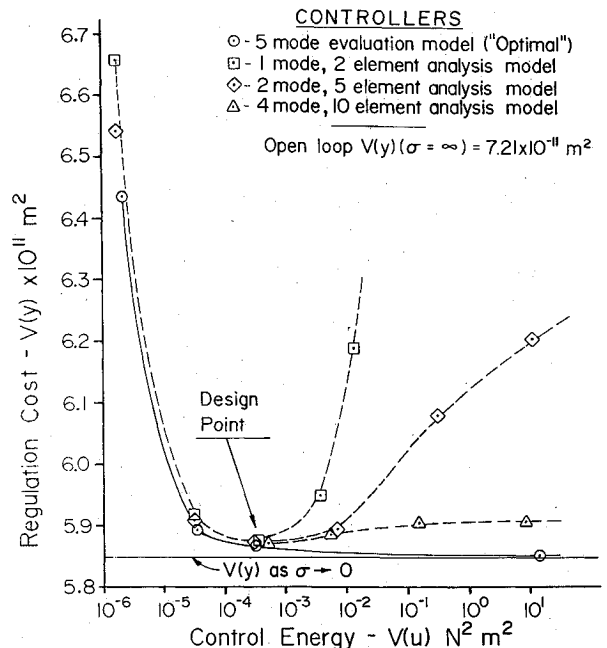


Fig. 12 Performance plot: three reduced order controllers.

The regulation cost  $V(y)$  and control energy  $V(u)$  are calculated as follows:

$$\begin{aligned}
 V(y) &= \lim_{t \rightarrow \infty} \frac{1}{t} E \int_0^t \|y(\tau)\|_Q^2 d\tau \\
 &= \text{tr}[C_E]^T [Q] [C_E] [X_{11}] \\
 V(u) &= \lim_{t \rightarrow \infty} \frac{1}{t} E \int_0^t \|u(\tau)\|_R^2 d\tau \\
 &= \text{tr}[G]^T [R] [G] [X_{22}]
 \end{aligned} \quad (26)$$

where  $[X]$  satisfies

$$\begin{aligned}
 [X] [A_a]^T + [A_a] [X] + [D_a] [W_a] [D_a]^T &= \bar{Q} \\
 [W_a] &= \begin{bmatrix} W & 0 \\ 0 & V \end{bmatrix} \\
 [X] &= \begin{bmatrix} X_{11} & X_{21}^T \\ X_{21} & X_{22} \end{bmatrix}
 \end{aligned} \quad (27)$$

For this example, both  $[Q]$  and  $[R]$  equal 1.0.

The evaluation process proceeds as follows. For a given reduced-order design model, a set of reduced-order controllers dependent upon the control weighting parameter  $\sigma$  is designed. These controllers are used to close the evaluation model loop and calculate a set of regulation cost vs control energy values. Finally, a full-order controller using the evaluation model itself as the control design model is designed. This serves as a comparison for the performance of the reduced-order models. The resulting controller will be optimal, while the controllers designed using the reduced-order control design models will not be. The resulting performance plots of regulation cost vs control energy will have the form shown in Fig. 2. The plot has a limiting value for regulation cost.  $V(y) (\sigma \rightarrow 0)$  is the lowest possible regulation cost value regardless of controller effort. This value is nonzero due to errors in reconstructing the state. Now, for the reduced-order controllers, the regulation cost will decrease as  $\sigma \rightarrow 0$ , then increase. This is due to the controllability and observability of those higher modes not included in the control design model.

A performance plot for the models in Table 2 has been calculated and is shown in Fig. 12. As expected, all reduced-order controllers are able to increase the performance of the system for low control effort. As control effort increases, however, system performance is degraded. The performance of all the reduced models, however, is exceptional. The one-mode, reduced-order controller achieves a minimum regulation cost of  $5.87 \times 10^{-11} \text{ m}^2$  before it begins to diverge from the optimal controller. When compared with the best theoretical system regulation cost of  $5.8497 \times 10^{-11} \text{ m}^2$ , this controller has an error in regulation cost of only 0.4%. The other two reduced-order controllers perform better at higher control energies, but only slightly better at the "design point." Although, in general, the design point is a function of controller order, it is not in this case, since the first mode dominates the dynamic behavior of the lattice. It was also expected that for low values of  $\sigma$ , the controllability of the truncated modes would drive the system unstable as the control effort approaches infinity ( $\sigma \rightarrow 0$ ). All of the closed loop systems were still stable, however, for  $\sigma$  as small as  $\sigma = 1.0 \times 10^{-25}$ .

### Conclusions

A basic procedure for simple and efficient finite element modeling of flexible beam-like lattice structures with repetitive

geometry has been developed. The formulation is based on the strain and kinetic energies of an equivalent continuum. The method is general and is not restricted to the particular lattice geometry studied here. Although the example lattice studied contains 10 repeating cells, the method is particularly suited to cases in which the number of repeating cells is considerably more than 10. The method will yield accurate results as long as there are a sufficient number of repeating cells per half-wavelength of a model. Furthermore, the method can be extended in a straightforward manner to plate- and shell-like lattice structures.

The present finite element analysis models allow the application of control theory to actual lattice structures in the form of the simple models. It has been common that the controls analyst has worked mostly with homogeneous isotropic finite element formulations or with large truss bar element models. The simple analysis models developed here present a modeling alternative. Using these models, free vibration analyses and preliminary control law design for beam-like lattice structures can be performed efficiently. The present formulation is also expected to be useful in the optimization of sensor/actuator locations, the minimization of structural mass, etc.

Specifically, this study has used the simple finite element formulation in the control design process for a typical lattice beam. Modal truncation has been applied to these simple analysis models using Modal Cost Analysis, a standard model reduction technique. The reduced-order models resulting from modal truncation have been used in the control law design process. The example chosen has shown that the structural modeling problem and the control design problem are not separable, since the model reduction process is influenced by the control objectives. This study has demonstrated a fundamental procedure for the integration of the structural modeling and control modeling problems which usually proceed separately.

### Acknowledgments

This work was sponsored under Air Force Office of Scientific Research Contract AFOSR-83-0104 administered by Dr. Anthony Amos.

### References

- <sup>1</sup>Noor, A.K., Anderson, M.S., and Greene, W.H., "Continuum Models for Beam- and Plate-like Lattice Structures," *AIAA Journal*, Vol. 16, Dec. 1978, pp. 1219-1228.
- <sup>2</sup>Berry, D.T., Yang, T.Y., and Skelton, R.E., "Dynamics and Control of Lattice Beams Using Complex and Simplified Finite Element Models," *AIAA Paper 84-1043*, May 1984.
- <sup>3</sup>Archer, J.S., "Consistent Matrix Formulations for Structural Analysis Using Finite Element Techniques," *AIAA Journal*, Vol. 3, Oct. 1965, pp. 1910-1918.
- <sup>4</sup>Przemienicki, J.S., *Theory of Matrix Structural Analysis*, McGraw Hill Book Co., New York, 1968.
- <sup>5</sup>Blevins, R.D., *Formulas for Natural Frequencies and Mode Shape*, Van Nostrand Reinhold, New York, 1979, pp. 180-181.
- <sup>6</sup>Berry, D.T., "Feedback Control, Large Amplitude Vibration, and Postbuckling of Space Lattice Beams Using Simplified Finite Element Models," M.S. Thesis, Purdue University, West Lafayette, Ind., May 1985.
- <sup>7</sup>Skelton, R.E. and Gregory, C.Z., "Measurement Feedback and Model Reduction by Modal Cost Analysis," *Proceedings of the Joint Automatic Control Conference*, Denver, 1979, pp. 211-218. (See also, Skelton, R.E. and Hughes, P.C., "Modal Cost Analysis for Linear Matrix-Second-Order Systems," *Journal of Dynamic Systems, Measurement and Control*, Vol. 102, Sept. 1980, pp. 151-158.)
- <sup>8</sup>Skelton, R.E., Hughes, P.C., Hablani, H.B., "Order Reduction for Models of Space Structures Using Modal Cost Analysis," *Journal of Guidance, Control, and Dynamics*, Vol. 5, July-Aug. 1982, pp. 351-357.
- <sup>9</sup>Kwakernaak, H., Sivan, R., *Linear Optimal Control Systems*, John Wiley & Sons, New York, 1982, Chap. 5.